GEOLOGY | THE GEOLOGICAL SOCIETY OF AMERICA®

https://doi.org/10.1130/G50385.1

Manuscript received 10 February 2022
Revised manuscript received 25 June 2022
Manuscript accepted 6 July 2022

Published online 31 August 2022

Trench retreat recorded by a subduction zone metamorphic history

Jie Dong[1], Marty Grove[2], Chunjing Wei[1]*, Bao-Fu Han[1]*, An Yin[3], Jiafu Chen[4], Ang Li[1] and Zhicheng Zhang[1]
[1]MOE Key Laboratory of Orogenic Belts and Crustal Evolution, School of Earth and Space Sciences, Peking University, Beijing 100871, China
[2]Department of Geological Sciences, Stanford University, Stanford, California 94305, USA
[3]Department of Earth, Planetary, and Space Sciences, University of California, Los Angeles, California 90095-1567, USA
[4]Department of Geology, Northeastern University, Shenyang 110819, China

ABSTRACT

Upper amphibolite-facies metamorphism in subduction zone rocks may occur under exceptional tectonic settings. Differentiating competing mechanisms for its occurrence requires carefully integrated, high-resolution thermobarometric and geochronologic studies of mélange rocks with well-defined field relationships. We present new pressure, temperature, and age data from the classic Cretaceous Catalina Schist in southern California (USA) that allow us to establish a plausible model for its high-temperature metamorphic history. Our results indicate that garnet-amphibolite blocks in the structurally highest amphibolite-facies mélange preserve evidence of three stages of tectonic evolution: (1) prograde lawsonite eclogite-facies metamorphism that peaked at 2.4–2.7 GPa with temperatures >580 °C during fixed-trench subduction (120–115 Ma); (2) post-peak epidote eclogite-facies metamorphism followed by amphibolite-facies metamorphism at 1.4–1.3 GPa with temperatures of 740–790 °C during trench retreat (115–105 Ma); and (3) isothermal decompression (1.3 GPa to <1.0 GPa at temperatures of 780 °C) and cooling during trench advance and slab-flattening subduction (ca. 105–100 Ma). Our model implies the presence of a continuous Cordilleran subduction system in the Cretaceous, which had varying tectonic regimes through episodes of trench retreat/advance and slab shallowing/steepening that, in turn, dictated the development of the Cordilleran arc system.

INTRODUCTION

Plate convergence associated with the advance, retreat, and fixed position of trenches (Lallemand et al., 2008) and slab steepening/flattening produces different pressure–temperature–time (*P-T-t*) histories of subduction zone rocks (e.g., Gerya and Meilick, 2011; Faryad and Cuthbert, 2020; Peacock, 2020). Fixed-trench subduction results in a steady-state thermal structure of the subduction zone. Alternatively, trench advance subduction causes subduction zone cooling, while trench retreat or slab steepening heats up the subduction zone. This simple framework permits evaluation of evolving and/or superposed modes of subduction along an ancient suture zone if its tectonothermal history can be established. We demonstrate how the mid-Cretaceous convergence history of the North American Cordillera in southern California (USA) can be deduced from existing and new data collected from the anomalously high-temperature amphibolite-facies unit within the classic, subduction-related Catalina Schist (e.g., Platt, 1975; Fig. 1).

GEOLOGICAL BACKGROUND

The Catalina Schist consists of downward-younging, structurally stacked metamorphic units that increase upward in age and metamorphic grade from lawsonite-albite to amphibolite facies (Fig. 1; Platt, 1975). At the highest structural level, amphibolite facies infiltration of aqueous fluids led to pervasive metasomatism, the formation of talc and chlorite-rich schist selvages around ultramafic and mafic protoliths, and partial melting of mafic blocks (Platt, 1975; Sorensen and Barton, 1987; Bebout and Barton, 2002; Penniston-Dorland et al., 2014; Harvey et al., 2021a; Fig. 1). These previous studies have all reported partial preservation of precursor eclogitic assemblages, which consist of garnet–rutile–clinopyroxene (20–35% jadeite component) in mafic block interiors, but their *P-T* evolution has not been well addressed.

The aforementioned amphibolite-facies metamorphism occurred at 122–111 Ma based on U-Pb metamorphic zircon ages, garnet Lu-Hf/Sm-Nd ages, and the youngest detrital zircon ages from amphibolite-facies metasediments (Mattinson, 1986; Anczkiewicz et al., 2004; Grove et al., 2008; Page et al., 2019; Harvey et al., 2021b). Cooling to ~400 °C proceeded until 105–100 Ma based on $^{40}Ar/^{39}Ar$ hornblende and muscovite ages (Grove and Bebout, 1995). The structurally lower blueschist unit was accreted after ca. 97 Ma based on the youngest detrital zircon ages (Grove et al., 2008). The Catalina Schist was ultimately exhumed to the surface during middle Miocene rifting of the former forearc region that formed the inner southern California borderland (Crouch and Suppe, 1993; Fig. 1).

PETROGRAPHY AND METAMORPHIC *P–T–t* EVOLUTION

We collected two samples (CA20–1 and CA20–2) from garnet amphibolite blocks in a chlorite-dominated mélange (33°24′3.59″N, 118°24′57.60″W) (Fig. 1). Methods for determining bulk-rock and mineral compositions, U-Pb zircon and rutile ages, trace element concentrations in zircon, garnet, and titanite, and phase equilibria calculations are described in the Supplemental Material[1].

*E-mails: cjwei@pku.edu.cn; bfhan@pku.edu.cn

[1]Supplemental Material. Supplemental text, Figures S1–S9, and Tables S1–S5. Please visit https://doi.org/10.1130/GEOL.S.20466123 to access the supplemental material, and contact editing@geosociety.org with any questions.

CITATION: Dong, J., Grove, M., Wei, C., Han, B.-F., Yin, A., Chen, J., Li, A., and Zhang, Z., 2022, Trench retreat recorded by a subduction zone metamorphic history: Geology, v. 50, p. 1281–1286, https://doi.org/10.1130/G50385.1

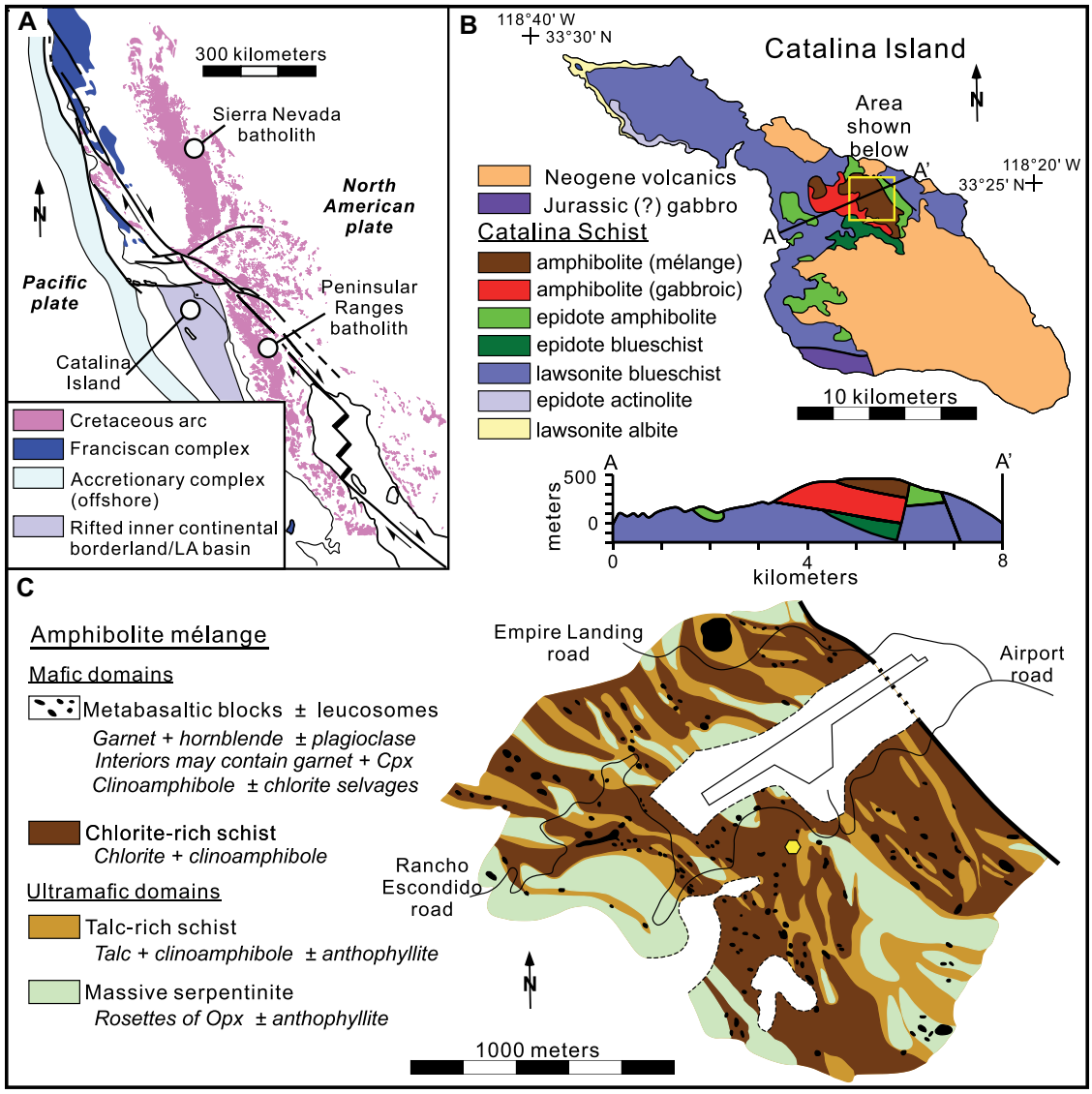

Figure 1. Tectonic setting of the Catalina Schist (southern California, USA). (A) California and Baja California margin showing the dominantly 130–85 Ma Sierra Nevada and Peninsular Ranges batholiths and corresponding subduction zone rocks (Franciscan Complex). Accretionary complex is offshore in southern California. The Catalina Schist was exhumed from beneath the Peninsular Ranges forearc during middle Miocene rifting that formed the inner continental borderland and Los Angeles (LA) basin (Crouch and Suppe, 1993). (B) Geologic map and cross section of Catalina Island, modified after Platt (1975) and Grove et al. (2008) showing a stacked sequence of metamorphic units in the Catalina Schist. (C) Map of the amphibolite-facies mélange, modified after Bebout and Barton (2002); the sampling location is marked by a yellow hexagon.

Sample CA20–2 consists of garnet, clinopyroxene, amphibole, epidote, plagioclase, titanite, accessory quartz, rutile, and apatite (Fig. 2A; Figs. S1A and S1B in the Supplemental Material). Garnet exhibits complex core–mantle–rim zoning in both major and rare earth elements (REEs) (Figs. 2D and 2E; Fig. S2). The zoning profile X_{Prp} [Mg / (Ca + Mg + Fe + Mn)] first increases outward in the core (C1a/C1b) and inner rim (R1a), followed by an outward decrease in the mantle (MT1) and outer rim (R1b) (Fig. 2D). Correspondingly, the concentration of heavy rare earth elements (HREEs) decreases away from the core, whereas that of the medium REEs (MREEs) increases from the mantle toward the rim (Fig. 2E). Omphacitic clinopyroxene is replaced by diopside-plagioclase symplectites (Fig. 2B). These textures yield an integrated X_{Na} [Na/(Na + Ca)] of 0.23–0.24 (Fig. S3B). Amphibole is hornblende-edenite with Ti contents of 0.06–0.10 per formula unit (p.f.u.) (Figs. S3C and S3D). Sample CA20–1 has a similar mineral assemblage (Fig. S1C) and garnet zoning pattern (Fig. S3A). Numerous rectangle or box-shaped multiphase inclusions occur inside garnet, all of which contain epidote and chlorite ± phengite (Si = 3.44–3.45 p.f.u.), quartz, titanite/rutile, and albite. We interpret these assemblages as pseudomorphs that formed through lawsonite breakdown (Fig. 2C; Fig. S4; Hamelin et al., 2018), which is consistent with the report of lawsonite by Penniston-Dorland et al. (2014) from similar garnet amphibolites.

Phase relationships calculated using THERMOCALC (e.g., Holland and Powell, 1998) are shown in Figures S5–S7. Three metamorphic stages are summarized in Figure 3. In stage 1 (I in Fig. 3), major element zoning (e.g., X_{Prp} and X_{Grs}) in the garnet core (Fig. 2D; Fig. S3A) indicates a prograde path from 1.8–2.2 GPa and $T < 510$°C to the peak *P-T* condition of 2.4–2.7 GPa and >580°C in the lawsonite eclogite field, consistent with the interpreted earlier occurrence of lawsonite and the highest Si content in phengite from sample CA20–1 (Fig. 3). This prograde evolution caused significant growth of garnet and devolatilization via lawsonite and chlorite breakdown (Fig. S5C) and is consistent with the REE zoning patterns in the garnet core (Fig. 2E). Major element zoning in the garnet mantle and the integrated X_{Na} in clinopyroxene indicate that the initial phase of stage 2 (solid IIa path in Figures 3 and S5B) involved decompression to epidote eclogite facies conditions of 1.9–1.8 GPa and 600–615°C. Overprinting of the former eclogitic assemblages by amphibole occurred at the expense of garnet, chlorite, and clinopyroxene (Fig. S5C). The advanced phase of stage 2 (IIb in Fig. 3) involved decompressional heating to 1.4–1.3 GPa and 740–790 °C. This is constrained by the major element zoning in the garnet mantle and inner rim, Ti in amphibole, and Zr-in-titanite thermometry (Fig. S6). Although the garnet mantle zoning of major elements was likely impacted by diffusion, REE zoning is well-preserved and may represent further prograde growth at higher *P-T* conditions (the path segment is denoted by the question mark in Figure 3 and Figure S5B). In the culmination of stage IIb,

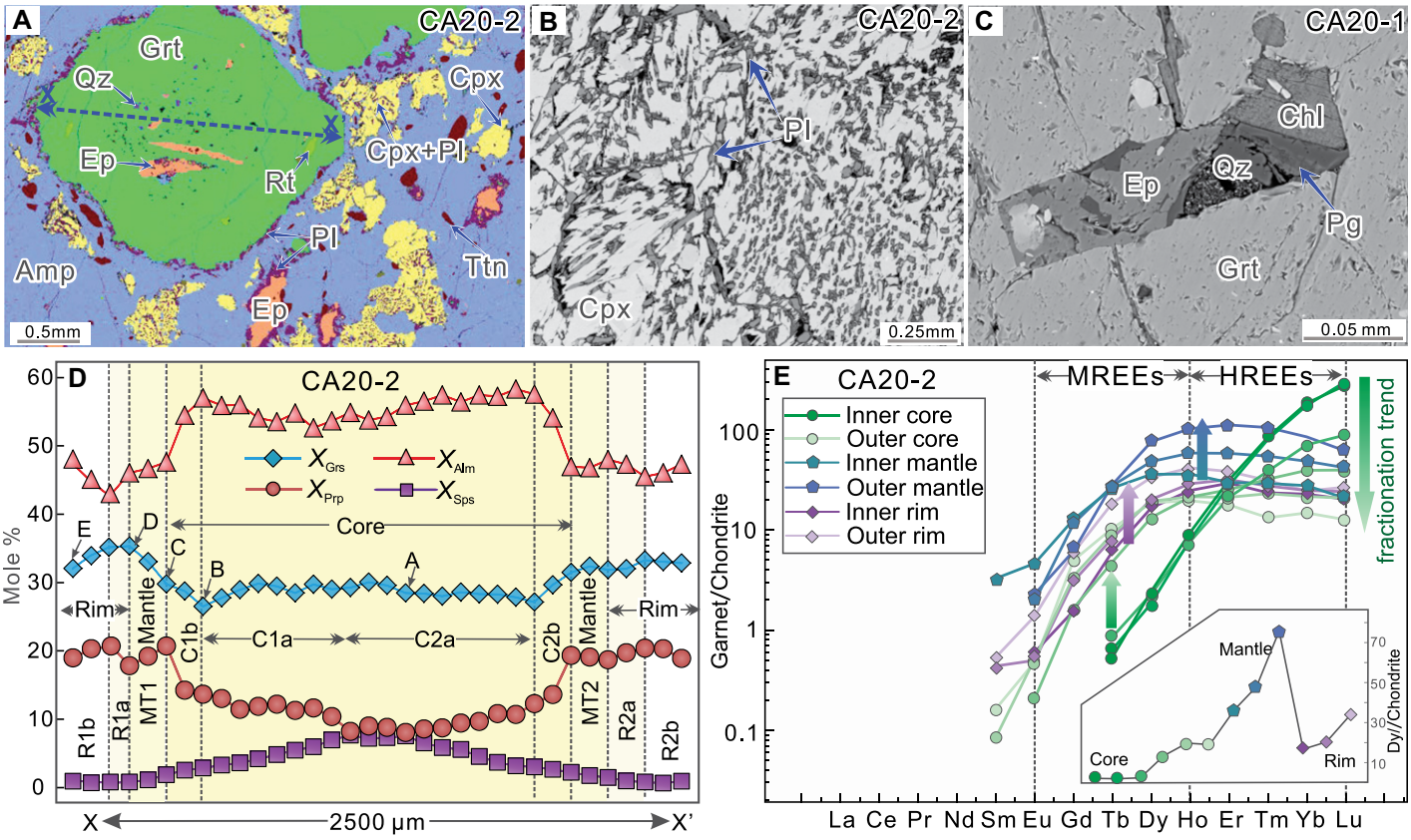

Figure 2. (A–C) Microtextures of garnet amphibolite samples, and chemical zoning profiles of (D) major elements and (E) rare earth elements (REEs) for garnet. (A) A phase image showing garnet porphyroblasts surrounded by plagioclase (Pl) and amphibole (Amp). (B) Clinopyroxene (Cpx) is replaced by diopside-plagioclase (Pl) symplectites. (C) Rectangle-shaped multiphase inclusions of paragonite (Pg), chlorite (Chl), epidote (Ep), and quartz (Qz) in garnet (Grt) core. MREE—middle rare earth elements; HREE—heavy rare earth elements; Rt—rutile; Ttn—titanite.

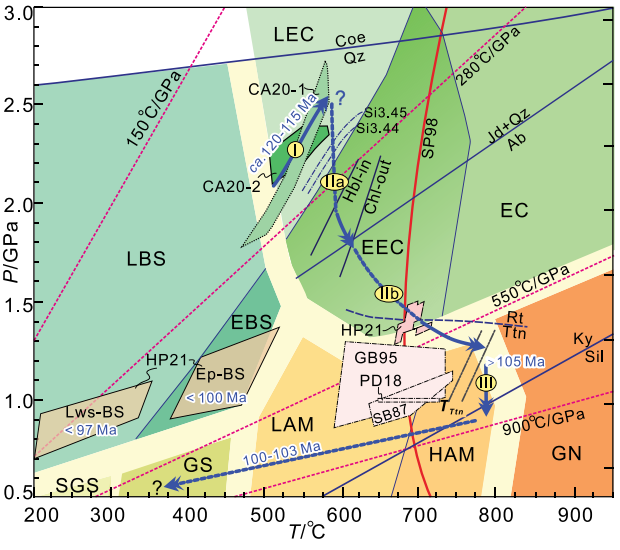

Figure 3. Pressure-temperature-time (*P-T-t*) evolution of the garnet amphibolite unit from the Catalina Schist (southern California, USA). Stage I: early prograde to peak-pressure eclogite facies. Stage II: post-peak decompression and heating involving an early decompression-dominant substage (IIa) and a late heating-dominant substage toward the peak temperature (IIb). Stage III: further isothermal decompression. Previous results from the amphibolite mélange are shown for comparison (SB87, Sorensen and Barton, 1987; GB95, Grove and Bebout, 1995; PD18, Penniston-Dorland et al., 2018; HP21, Harvey et al., 2021a). The Rt/Ttn, Hbl-in, and Chl-out curves are from Figure S5B (see footnote one) and the Si3.44/Si3.45 curves are from Figure S7. The fluid-saturated solidus (SP98) of a metabasic rock and metamorphic facies variations are from Wei and Duan (2019). The T_{Ttn} curves are defined by Zr-in-titanite thermometry (Table S5). (S)GS—(sub)greenschist facies; L/EBS—lawsonite/epidote blueschist facies; L/HAM—low-/high-temperature amphibolite facies; GN—granulite facies; L/EEC—lawsonite/epidote eclogite facies; EC—lawsonite/epidote-free eclogite facies. Ab—albite; Chl—chlorite; Coe—coesite; Hbl—hornblende; Ky—kyanite; Jd—jadeite; Rt— rutile; Sil—sillimanite; Ttn—titanite; Qz—quartz.

REE patterns from the inner rim of garnet are consistent with amphibole and epidote dehydration melting in the upper amphibolite facies (Fig. S5C). Finally, in stage 3 (III in Fig. 3), zoning of major elements in the outer rim of garnet and the growth of plagioclase indicate a near-isothermal decompression path to <1.0 GPa at ~780°C followed by subsequent cooling.

U-Pb dating yields metamorphic zircon ages of 120–104 Ma. The oldest age of 119.7 ± 2.3 Ma (Fig. S8B) is consistent with detrital zircon U-Pb results from amphibolite-facies metasedimentary rocks younger than 122 ± 3 Ma (Grove et al., 2008). The combined U-Pb zircon ages and trace element data show that $(Lu/Gd)_N$ (N—normalized) ratios and MREE abundance in zircon decrease and increase, respectively, with decreasing zircon age (Fig. S8C). This correlation indicates that metamorphic zircon crystallization occurred during the growth of garnet and the breakdown of MREE-rich phases such as titanite, lawsonite, epidote, and amphibole (Konrad-Schmolke et al., 2008; Martin et al., 2014). We interpret the prevalent 115 Ma zircon U-Pb age, garnet Lu-Hf/Sm-Nd age, and hornblende $^{40}Ar/^{39}Ar$ ages previously reported for the Catalina garnet

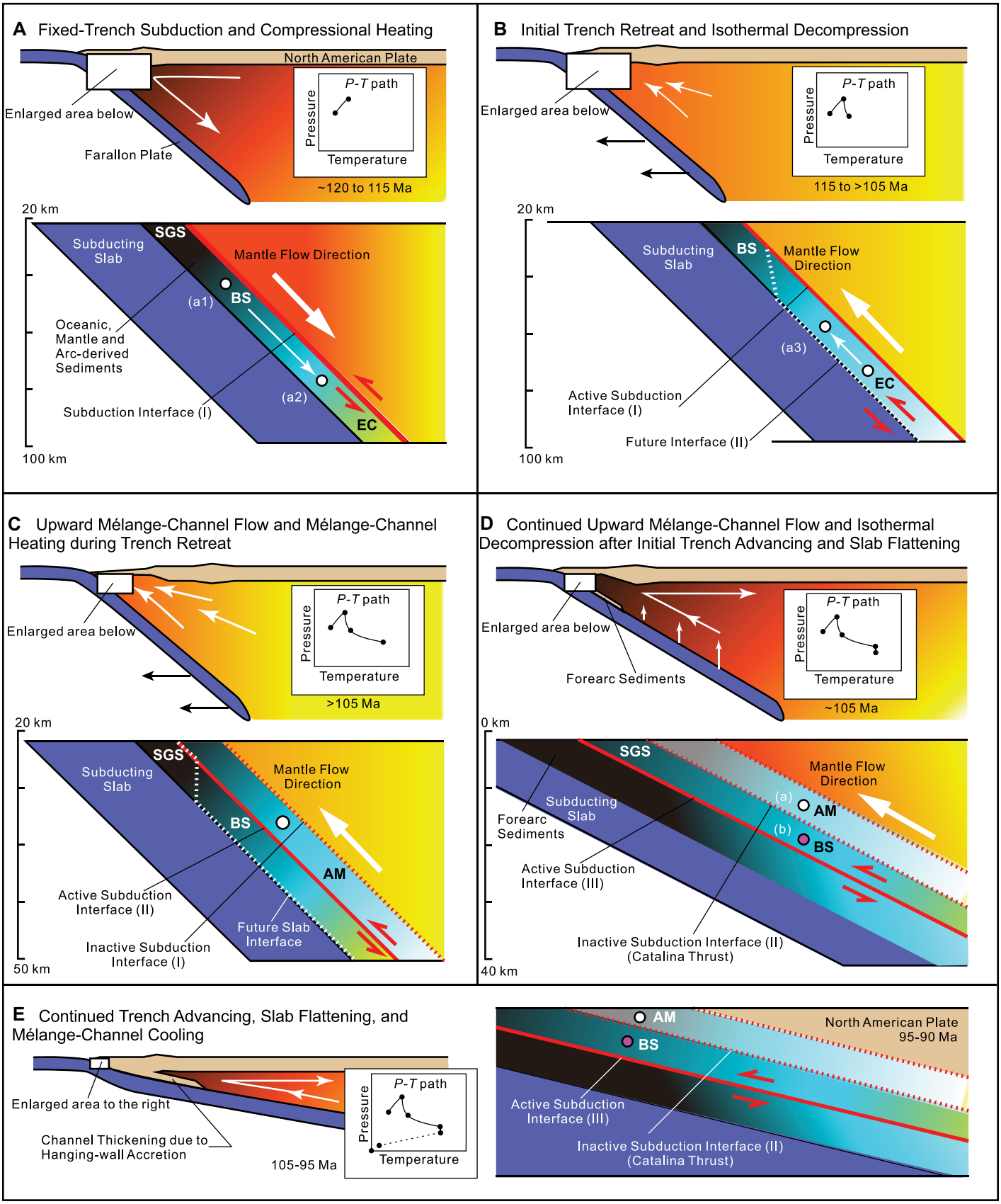

Figure 4. Tectonic model of the Catalina Schist (southern California, USA) showing (A) fixed-trench subduction; (B) initial trench retreat; (C) upward mélange channel flow and heating during trench retreat; (D) continued upward mélange channel flow and isothermal decompression after initial trench advance and slab flattening; and (E) trench advance, slab flattening, and cooling of the mélange channel. SGS—(sub) greenschist facies; BS—blueschist facies; AM—amphibolite facies.

amphibolites (Mattinson, 1986; Anczkiewicz et al., 2004; Grove et al., 2008; Page et al., 2019) as marking the onset of amphibolization during stage II decompression. The 115–104 Ma metamorphic zircon growth likely occurred during the final phase of stage IIb and may have been linked to the renewed garnet growth. Finally, the U-Pb rutile ages (103 ± 2 Ma) (Fig. S8D) are consistent with $^{40}Ar/^{39}Ar$ muscovite ages that record the end of the post-stage III cooling history (Grove et al., 2008).

DISCUSSION AND CONCLUSIONS

The metamorphic history we have determined for garnet-amphibolite blocks in the structurally highest amphibolite-facies mélange unit of the Catalina Schist can be interpreted in terms of advance/retreat of the trench and shallowing/steepening of subducting oceanic crust during the emplacement of the Catalina Schist (Fig. 4). Prograde lawsonite eclogite-facies metamorphism during stage 1 occurred during fixed-trench subduction (120–115 Ma) (Fig. 4A) (e.g., Peacock, 2020). Stage 2 involved post-peak decompression to epidote eclogite-facies conditions and ultimately decompression heating to upper amphibolite facies during trench retreat, slab steepening, and mantle upwelling (115–105 Ma) (Figs. 4B and 4C) (e.g., Butler and Beaumont, 2017). Finally, late-stage decompression and cooling (stage 3) was caused by trench advance and slab flattening (ca. 105–100 Ma; Figs. 4D and 4E). Our model is compatible with other proposed instances of decompressional heating linked to slab rollback within subduction zones (e.g., Avellaneda-Jiménez et al., 2020; Faryad and Cuthbert, 2020) and consistent with continuous subduction astride the coeval and adjacent 130–90 Ma Peninsular Ranges arc. The latter experienced mafic mantle input that was coeval with its early extensional history and relocated to the east due to compression and was genetically related to the Catalina Schist after ca. 105 Ma (Gastil et al., 1981; Busby, 2004).

Our *P-T* results (Fig. 3) indicate that the peak temperatures are ~50 °C higher than previous Grt-Cpx geothermometry suggested (Sorensen and Barton, 1987), possibly due to different activity models and/or Fe–Mg diffusion (Pattison et al., 2003). More significantly, the peak pressure (2.4–2.7 GPa) is appreciably higher than the 1.26–1.44 GPa defined by the quartz-in-garnet elastic barometer (Harvey et al., 2021a). This discrepancy can be explained by viscous relaxation under high-temperature conditions (Moulas et al., 2020). Preservation of omphacitic clinopyroxene in the mafic blocks that we sampled indicates that metasomatic recrystallization minimally affected our samples (e.g., Sorensen and Barton, 1987; Bebout and Barton, 2002; Fig. 1C). Similarly, melt extraction of <5 mol% during anatexis exerts a negligible effect on the estimated peak-pressure conditions (Fig. S9).

The nascent-subduction model of Platt (1975) attributed all units of the Catalina Schist to have formed beneath an initially hot and rapidly cooled mantle hanging wall. Platt's (1975) model was advanced to explain the Franciscan Mélange Complex of northern California, where amphibolite- and eclogite-facies tectonic blocks with counterclockwise *P-T* paths were formed at about the same time as the 170–160 Ma forearc-crust formation (Coast Ranges ophiolite) and Middle Jurassic arc magmatism in the Sierra Nevada (Cloos, 1985; Wakabayashi, 1990; Shervais et al., 2004; Tsujimori et al., 2007; Fig. 1). However, the nascent subduction model does not account for the following conditions: (1) the amphibolite-facies rocks overprinted former lawsonite eclogite assemblages, exhibiting clockwise rather than counterclockwise *P-T* paths; (2) an ~15–20 m.y. age gap separated the timing of the (slowly cooled) amphibolite- and (rapidly cooled) blueschist-facies metamorphism, and the amphibolite-facies rocks lack the blueschist-facies overprint that would be present had the two been formed in close proximity; and (3) the high-temperature metamorphism within the Catalina Schist occurred ~40 m.y. after formation of the overlying Middle Jurassic mafic forearc basement (Grove et al., 2008; Platt et al., 2020).

While forearc thrusting (Grove et al., 2008) explains diachronous formation of the structurally bounded Catalina Schist units, there is no compelling evidence that the mafic protolith of the amphibolite unit is the Middle Jurassic forearc basement as required by the model. Moreover, the shallow 120–105 Ma underthrusting of the Catalina Schist beneath the magmatic arc requires the amphibolite-facies rocks to have formed during prograde metamorphism, which is inconsistent with our *P-T* results. Finally, while oceanic ridge subduction can produce an upper amphibolite-facies overprint of the subduction complex (e.g., García-Casco et al., 2008), such a process can be ruled out by the continuous 130–90 Ma intrusive history of the adjacent 800-km-long Peninsular Ranges batholith (e.g., Grove et al., 2008).

Our continuous subduction model, in which the geometry of the subducting slab varied over time, provides the simplest explanation for amphibolite-facies metamorphism of the Catalina Schist (Fig. 4). This finding helps resolve key details regarding the development of the Catalina Schist and further demonstrates that crucial insights into subduction zone evolution can be produced from carefully integrated, high-resolution thermobarometric and geochronologic studies.

ACKNOWLEDGMENTS

This work was supported by the National Natural Science Foundation of China (grants 42102042 and 42030304). We thank Rob Strachan for encouragement and Antonio García-Casco and two anonymous reviewers for their constructive comments that greatly improved the original draft.

REFERENCES CITED

Anczkiewicz, R., Platt, J.P., Thirlwall, M.F., and Wakabayashi, J., 2004, Franciscan subduction off to a slow start: Evidence from high-precision Lu-Hf garnet ages on high grade-blocks: Earth and Planetary Science Letters, v. 225, p. 147–161, https://doi.org/10.1016/j.epsl.2004.06.003.

Avellaneda-Jiménez, D.S., Cardona, A., Valencia, V., León, S., and Blanco-Quintero, I.F., 2020, Metamorphic gradient modification in the Early Cretaceous Northern Andes subduction zone: A record from thermally overprinted high-pressure rocks: Geoscience Frontiers, v. 13, 101090, https://doi.org/10.1016/j.gsf.2020.09.019.

Bebout, G.E., and Barton, M.D., 2002, Tectonic and metasomatic mixing in a high-*T*, subduction-zone mélange—Insights into the geochemical evolution of the slab–mantle interface: Chemical Geology, v. 187, p. 79–106, https://doi.org/10.1016/S0009-2541(02)00019-0.

Busby, C., 2004, Continental growth at convergent margins facing large ocean basins: A case study from Mesozoic convergent-margin basins of Baja California, Mexico: Tectonophysics, v. 392, p. 241–277, https://doi.org/10.1016/j.tecto.2004.04.017.

Butler, J.P., and Beaumont, C., 2017, Subduction zone decoupling/retreat modeling explains south Tibet (Xigaze) and other supra-subduction zone ophiolites and their UHP mineral phases: Earth and Planetary Science Letters, v. 463, p. 101–117, https://doi.org/10.1016/j.epsl.2017.01.025.

Cloos, M., 1985, Thermal evolution of convergent plate margins: Thermal modeling and reevaluation of isotopic Ar ages for blueschists in the Franciscan Complex of California: Tectonics, v. 4, p. 421–433, https://doi.org/10.1029/TC004i005p00421.

Crouch, J.K., and Suppe, J., 1993, Late Cenozoic tectonic evolution of the Los Angeles Basin and inner California borderland; A model for core complex–like crustal extension: Geological Society of America Bulletin, v. 105, p. 1415–1434, https://doi.org/10.1130/0016-7606(1993)105<1415:LCTEOT>2.3.CO;2.

Faryad, S.W., and Cuthbert, S.J., 2020, High-temperature overprint in (U)HPM rocks exhumed from subduction zones; a product of isothermal decompression or a consequence of slab break-off (slab rollback)?: Earth-Science Reviews, v. 202, https://doi.org/10.1016/j.earscirev.2020.103108.

García-Casco, A., Lázaro, C., Rojas-Agramonte, Y., Kröner, A., Torres-Roldán, R.L., Núñez, K., Neubauer, F., Millán, G., and Blanco-Quintero, I., 2008, Partial melting and counterclockwise *P-T* path of subducted oceanic crust (Sierra del Convento mélange, Cuba): Journal of Petrology, v. 49, p. 129–161, https://doi.org/10.1093/petrology/egm074.

Gastil, R.G., Morgan, G.J., and Krummenacher, D., 1981, The tectonic history of peninsular California and adjacent Mexico, *in* Ernst, W.G., ed., The Geotectonic Development of California (Rubey Volume I): Englewood Cliffs, New Jersey, Prentice Hall, p. 284–306.

Gerya, T.V., and Meilick, F.I., 2011, Geodynamic regimes of subduction under an active margin: Effects of rheological weakening by fluids and melts: Journal of Metamorphic Geology, v. 29, p. 7–31, https://doi.org/10.1111/j.1525-1314.2010.00904.x.

Grove, M., and Bebout, G.E., 1995, Cretaceous tectonic evolution of coastal southern California: Insights from the Catalina Schist: Tectonics,

v. 14, p. 1290–1308, https://doi.org/10.1029/95TC01931.
Grove, M., Bebout, G.E., Jacobson, C.E., Barth, A.P., Kimbrough, D.L., King, R.L., and Gehrels, G.E., 2008, The Catalina Schist: Evidence for middle Cretaceous subduction erosion of southwestern North America, *in* Draut, A.E., et al., eds., Formation and Applications of the Sedimentary Record in Arc Collision Zones: Geological Society of America Special Paper 436, p. 335–361, https://doi.org/10.1130/2008.2436(15).
Hamelin, C., Brady, J.B., Cheney, J.T., Schumacher, J.C., Able, L.M., and Sperry, A.J., 2018, Pseudomorphs after lawsonite from Syros, Greece: Journal of Petrology, v. 59, p. 2353–2384, https://doi.org/10.1093/petrology/egy099.
Harvey, K.M., Penniston-Dorland, S.C., Kohn, M.J., and Piccoli, P.M., 2021a, Assessing P-T variability in mélange blocks from the Catalina Schist: Is there differential movement at the subduction interface?: Journal of Metamorphic Geology, v. 39, p. 271–295, https://doi.org/10.1111/jmg.12571.
Harvey, K.M., Walker, S., Starr, P.G., Penniston-Dorland, S.C., Kohn, M.J., and Baxter, E.F., 2021b, A mélange of subduction ages: Constraints on the timescale of shear zone development and underplating at the subduction interface, Catalina Schist (CA, USA): Geochemistry Geophysics Geosystems, v. 22, https://doi.org/10.1029/2021GC009790.
Holland, T.J.B., and Powell, R., 1998, An internally consistent thermodynamic data set for phases of petrological interest: Journal of Metamorphic Geology, v. 16, p. 309–343, https://doi.org/10.1111/j.1525-1314.1998.00140.x.
Konrad-Schmolke, M., Zack, T., O'Brien, P.J., and Jacob, D.E., 2008, Combined thermodynamic and rare earth element modelling of garnet growth during subduction: Examples from ultrahigh-pressure eclogite of the Western Gneiss Region, Norway: Earth and Planetary Science Letters, v. 272, p. 488–498, https://doi.org/10.1016/j.epsl.2008.05.018.
Lallemand, S., Heuret, A., Faccenna, C., and Funiciello, F., 2008, Subduction dynamics as revealed by trench migration: Tectonics, v. 27, TC3014, https://doi.org/10.1029/2007TC002212.
Martin, L.A.J., Hermann, J., Gauthiez-Putallaz, L., Whitney, D.L., Vitale Brovarone, A., Fornash, K.F., and Evans, N.J., 2014, Lawsonite geochemistry and stability—Implication for trace element and water cycles in subduction zones: Journal of Metamorphic Geology, v. 32, p. 455–478, https://doi.org/10.1111/jmg.12093.
Mattinson, J.M., 1986, Geochronology of high-pressure–low-temperature Franciscan metabasites: A new approach using the U-Pb system, *in* Evans, B.W., and Brown, E.H., eds., Blueschists and Eclogites: Geological Society of America Memoir 164, p. 95–106, https://doi.org/10.1130/MEM164-p95.
Moulas, E., et al., 2020, Calculating pressure with elastic geobarometry: A comparison of different elastic solutions with application to a calc-silicate gneiss from the Rhodope Metamorphic Province: Lithos, v. 378, https://doi.org/10.1016/j.lithos.2020.105803.
Page, F.Z., Cameron, E.M., Flood, C.M., Dobbins, J.W., Spicuzza, M.J., Kitajima, K., and Valley, J.W., 2019, Extreme oxygen isotope zoning in garnet and zircon from a metachert block in mélange reveals metasomatism at the peak of subduction metamorphism: Geology, v. 47, p. 655–658, https://doi.org/10.1130/G46135.1.
Pattison, D.R., Chacko, T., Farquhar, J., and McFarlane, C.R., 2003, Temperatures of granulite-facies metamorphism: Constraints from experimental phase equilibria and thermobarometry corrected for retrograde exchange: Journal of Petrology, v. 44, p. 867–900, https://doi.org/10.1093/petrology/44.5.867.
Peacock, S.M., 2020, Advances in the thermal and petrologic modeling of subduction zones: Geosphere, v. 16, p. 936–952, https://doi.org/10.1130/GES02213.1.
Penniston-Dorland, S.C., Gorman, J.K., Bebout, G.E., Piccoli, P.M., and Walker, R.J., 2014, Reaction rind formation in the Catalina Schist: Deciphering a history of mechanical mixing and metasomatic alteration: Chemical Geology, v. 384, p. 47–61, https://doi.org/10.1016/j.chemgeo.2014.06.024.
Penniston-Dorland, S.C., Kohn, M.J., and Piccoli, P.M., 2018, A mélange of subduction temperatures: Evidence from Zr-in-rutile thermometry for strengthening of the subduction interface: Earth and Planetary Science Letters, v. 482, p. 525–535, https://doi.org/10.1016/j.epsl.2017.11.005.
Platt, J.P., 1975, Metamorphic and deformational processes in the Franciscan Complex, California: Some insights from the Catalina Schist terrane: Geological Society of America Bulletin, v. 86, p. 1337–1347, https://doi.org/10.1130/0016-7606(1975)86<1337:MADPIT>2.0.CO;2.
Platt, J.P., Grove, M., Kimbrough, D.L., and Jacobson, C.E., 2020, Structure, metamorphism, and geodynamic significance of the Catalina Schist terrane, *in* Heermance, R.V., and Schwartz, J.J., eds., From the Islands to the Mountains: A 2020 View of Geologic Excursions in Southern California: Geological Society of America Field Guide 59, p. 165–195, https://doi.org/10.1130/2020.0059(05).
Sorensen, S.S., and Barton, M.D., 1987, Metasomatism and partial melting in a subduction complex Catalina Schist, southern California: Geology, v. 15, p. 115–118, https://doi.org/10.1130/0091-7613(1987)15<115:MAPMIA>2.0.CO;2.
Shervais, J.W., Kimbrough, D.L., Renne, P., Hanan, B.B., Murchey, B., Snow, C.A., Zoglman Schuman, M.M., and Beaman, J., 2004, Multi-stage origin of the Coast Range Ophiolite, California: Implications for the life cycle of supra-subduction zone ophiolites: International Geology Review, v. 46, p. 289–315, https://doi.org/10.2747/0020-6814.46.4.289.
Tsujimori, T., Liou, J.G., Coleman, R.G., Cloos, M., Carlson, W.D., and Gilbert, M.C., 2007, Finding of high-grade tectonic blocks from the New Idria serpentinite body, Diablo Range, California: Petrologic constraints on the tectonic evolution of an active serpentinite diapir, *in* Cloos, M., et al., eds., Convergent Margin Terranes and Associated Regions: A Tribute to W.G. Ernst: Geological Society of America Special Paper 419, p. 67–80, https://doi.org/10.1130/2007.2419(03).
Wakabayashi, J., 1990, Counterclockwise P-T-t paths from amphibolites, Franciscan Complex, California: Relics from the early stages of subduction zone metamorphism: The Journal of Geology, v. 98, p. 657–680, https://doi.org/10.1086/629432.
Wei, C.J., and Duan, Z.Z., 2019, Phase relations in metabasic rocks: Constraints from the results of experiments, phase modelling and ACF analysis, *in* Zhang, L., et al., eds., HP–UHP Metamorphism and Tectonic Evolution of Orogenic Belts: Geological Society, London, Special Publication 474, p. 25–45, https://doi.org/10.1144/SP474.10.

Printed in USA